A virtual phase CCD detector for synchrotron radiation applications

Brian Rodricks and Roy Clarke

Department of Physics, The University of Michigan, Ann Arbor, Michigan 48109

Robert Smither

Argonne National Laboratory, Argonne, Illinois 60439

Alain Fontaine

LURE, CNRS 91405 Orsay, France

(Received 25 August 1988; accepted for publication 17 April 1989)

A two-dimensional charge coupled device (CCD) detector, based on the Texas Instruments "virtual phase" CCD, has been developed for synchrotron radiation applications. Simultaneous near-edge and multilayer scattering experiments have been carried out with the detector on an energy-dispersive synchrotron beamline. The detector was used in an optical mode where the CCD element is coupled to a phosphor screen by a pair of focusing and demagnifying lenses. We report on the performance of the detector in this mode.

INTRODUCTION

Synchrotron radiation has become a very important scientific tool in a diverse range of applications from surface structure studies to medical imaging. Special characteristics such as the high degree of collimation and polarization, the brightness of the beam and its broad spectral range, have made experiments feasible that were hitherto impossible.[1] Other features, particularly the pulsed structure of the beam, are beginning to open up exciting new areas of time-resolved studies.[2,3]

A limiting factor in realizing the full potential of x-ray synchrotron facilities is the development of detectors which can take advantage of the high flux and temporal characteristics of the new sources. The construction of a new generation of ultrahigh brilliance sources, such as Argonne National Laboratory's 7-GeV Advanced Photon Source (APS) and the European Synchrotron Radiation Facility (ESRF), with undulator beams that are many orders of magnitude more intense than existing sources, will place even more stringent demands on future detection schemes.[3]

Charge coupled devices (CCDs) are emerging as a very promising technology for x-ray detectors where large dynamic range, high-spatial resolution, and fast data acquisition are called for.[4] These are among the most important requirements for experiments utilizing high-brilliance sources such as APS and ESRF. In addition, CCDs possess certain desirable features which make them very interesting for studies of time-dependent structural phenomena. The way in which a CCD detector is read out, by a combination of parallel row transfers ($\sim 50\,\mu$s/row) and serial pixel-to-pixel transfers ($\sim 6\,\mu$s/pixel), allows for a versatility of operation that is unmatched by any other detector design.[5,6] For example, two-dimensional full-frame (584×390 pixels) diffraction images can be integrated and read out in about a second. Alternately, the CCD can be used in a "streak camera" mode to record a sequence of time-resolved one-dimensional data sets on sub millisecond time scales.

In this article we describe the design of a two-dimensional CCD x-ray detector system recently developed at the University of Michigan. The "virtual phase" architecture of the CCD chip employed by the detector offers several advantages over other designs for synchrotron radiation experiments. These advantages will be emphasized in the following sections.

The layout of the article is as follows. In Secs. I and II, we present an overview of the detector design and its readout electronics. Section III describes coupling of the CCD to a phosphor screen and in Secs. IV and V we present some results demonstrating the performance of the detector in recent experimental runs at the LURE synchrotron facility.

I. OVERVIEW OF THE VIRTUAL PHASE CCD

In a CCD, the charge produced by incident visible photons or x rays is stored in an array of potential wells in the inversion layer of an MOS (metal-oxide-silicon) structure. In order to read out the device, charge is transferred along a row from pixel to pixel. This requires an asymmetric potential which is normally provided by a three-level gate-electrode structure.[7]

In an alternate approach to this standard three-phase readout method, Texas Instruments have introduced the so-called "virtual phase" CCD chip architecture.[8] The asymmetric well structure in this type of CCD is achieved by deep ion implants so that only a single level of external clocking electrodes is required (see Fig. 1). This results in higher device yields, significantly reducing the cost of manufacture. Also, this type of CCD is generally more efficient in front-side illumination because less of the incident energy is absorbed by the gate-electrode structure.

In addition to simpler readout electronics as a result of the single-phase operation, the virtual phase concept has distinct advantages relevant to its application for x-ray area detection. In particular, the buried channel implant electrodes promote low dark current and radiation hardness,[9]

 0034-6748/89/082586-06$01.30

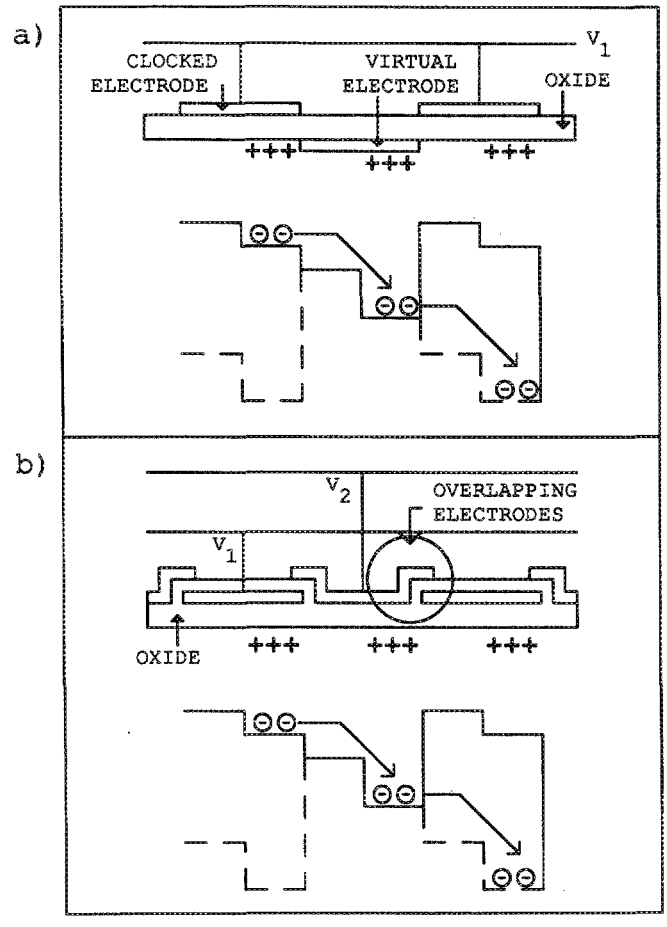

FIG. 1. Profile view of the physical structure and electrical potentials in two CCD architectures: (a) Texas Instruments virtual phase design; (b) standard two-phase design.

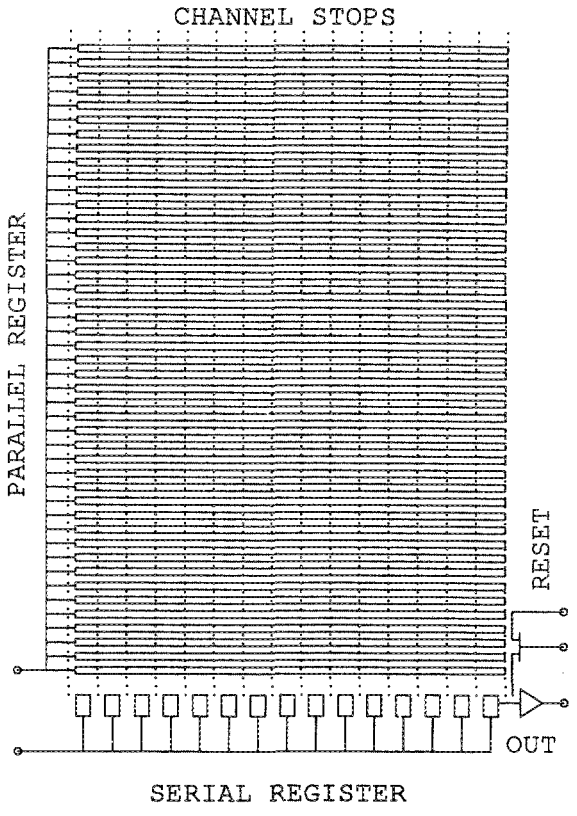

FIG. 2. Schematic view of the electrode structure of virtual phase CCD.

the latter feature being of importance when the CCD is used for direct imaging of x rays.[10]

The CCD used in the present detector is the TI4849 chip[11] consisting of 584 rows of pixels arranged in 390 columns. Each pixel is 22.4-μm square with a depletion depth of 12 μm; the relatively large depletion depth is well matched to direct exposure by x rays in the energy range 5–7 keV.

Figure 2 shows schematically the overall chip structure. During readout each row of stored charges is transferred to the serial register by means of the parallel electrode. The charge from each pixel is then transferred sequentially by the serial clock to a floating diffusion amplifier situated at the side of the gate electrode array. The on-chip amplifier response is approximately 1 $\mu V/e^-$.

II. DETECTOR READOUT ELECTRONICS

A detailed account of the readout, electronics has been reported previously.[12] Here we summarize the overall method of operation of the detector system. Figure 3 is a block diagram of the main components of the detector electronics, consisting of readout waveform generators, analog-digital converter (ADC), buffer memory, clock synchronization modules, and local fast LSI-11-based microprocessor control. Global control is handled by a Microvax II computer. Each of the local control functions are supported by CAMAC modules connected by a common bus.

The readout waveform generators, consisting of serial, parallel, and reset modules are fully programmable. This permits modifications to the amplitude and shape of individual waveforms interactively by means of the system software, a useful feature which helps to optimize the charge transfer efficiency (CTE).[12] This is particularly important when the CCD is exposed directly to x rays, in which case the effects of radiation damage may be corrected, to some extent, by waveform adjustments.

The output from the on-chip amplifier is sent through a low-noise preamplifier with a gain of 5. This preamplified signal is further amplified by an additional factor of 10 before processing in a correlated double-sampling circuit[12] which significantly reduces noise associated with the periodic reset signal for the on-chip amplifier. After a final state of amplification the correlated signal is digitized by a 12-bit ADC operating at 156 kHz. The overall gain of the system is 1000. The choice of a 12-bit ADC module here is a compromise between resolution [4096 analog—digital units (ADU)] and speed; the ADC is the limiting factor in readout time for the CCD. Finally, the digitized CCD readout signal is stored in a 1-Mbyte buffer memory.

The LSI-11 microprocessor initiates fast clear, integration, and readout operations of the CCD. The integration time can be set on line from a few microseconds to more than 10 s using a programmable delay gate generator. The micro-

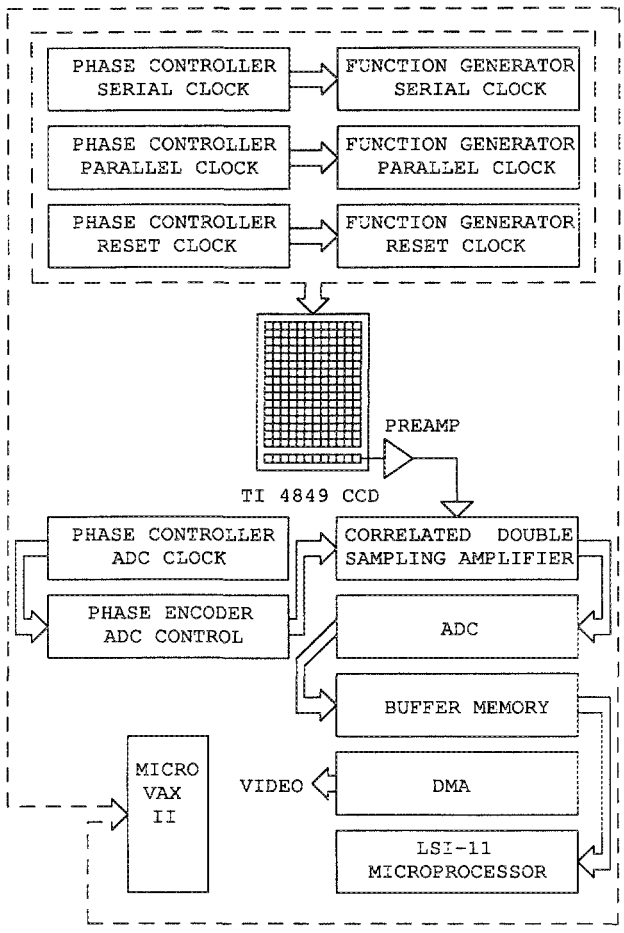

FIG. 3. Block diagram of CCD control and readout system.

processor is also provided with a direct memory access (DMA) channel to a high-resolution color monitor where a pixel map of the CCD chip can be displayed. Intensity profiles through any desired row, and pulse height histograms, are also possible using the graphics software. To be able to preview the data on line before it is stored on disk is very important for diagnostic purposes. The question of data handling for a system which acquires data at rates in excess of 1 Mbyte s^{-1} is an important aspect of the overall detector design. The current design has addressed this issue by permiting new macro programs to be downloaded into the LSI-11 CAMAC module; every aspect of the detector control electronics is accessible from menu-driven routines selected from the Microvax master terminal.

III. OPTICAL COUPLING TO PHOSPHOR SCREEN

The CCD detector can be used either for direct imaging of x rays or as an integrating camera to record a high-resolution image of x rays incident on a phosphor screen. Our immediate application, as a position sensitive detector for near-edge spectroscopic and scattering studies, required a larger sensing area than the actual size of the CCD chip (13×8.5 mm^2). In order to extend the effective diameter of the detector, we employed optical coupling of the chip to a 40-mm diam phosphor screen (Fig. 4). The phosphor screen is a Gd_2O_2S:Tb (P 43) phosphor (Trimax 2)[13] of thickness 80 μm. Images on this screen are focused onto the CCD chip using two back-to-back Nikon photographic lenses. A 50-mm/F 1.2 lens is coupled to the quartz window of the vacuum chamber containing the CCD chip and a 200 mm/F 4 lens is coupled to the phosphor. The resulting compound lens system gives demagnification of 4:1 on the CCD.

In order to reduce thermal carrier generation in the CCD, which can be a significant source of background noise, the chip was thermoelectrically cooled to $-50\,^{\circ}C \pm 0.2\,^{\circ}C$ using a three-stage thermoelectric cooling device.[14]

IV. PERFORMANCE OF THE DETECTOR: EXPERIMENTAL SETUP

A series of experiments using the virtual phase CCD detector have been performed at the LURE synchrotron radiation facility (Orsay, France) on an energy dispersive beamline. The purpose of the experiments was to investigate the glancing-angle reflectivity from platinum-carbon multilayer samples when the incident beam is close to an absorption edge of the platinum layers (L_{III}; 11.563 keV). Under these conditions a number of interesting issues can be addressed, including anomalous diffraction, surface standing waves, and reflection EXAFS (extended x-ray absorption fine structure). In addition, because the samples are multilayers, there is the possibility to study reflectivity behavior when the Bragg diffraction from the artificial layering occurs at glancing angles comparable to those for total external reflection. A two-dimensional detector, which probes simultaneously the scattering as a function of energy (E), and scattering wave vector (q) is particularly advantageous for this type of experiment.

The multilayer studies were performed using a triangular shaped Si(311) monochromater crystal, bent in order to vary continuously the incidence angle of the synchrotron x-ray beam spread over 1 mrad (see Fig. 5).[15] This arrangement yields a spatially dispersed beam of photons with a continuous spread of energies. The curvature of the bent Si

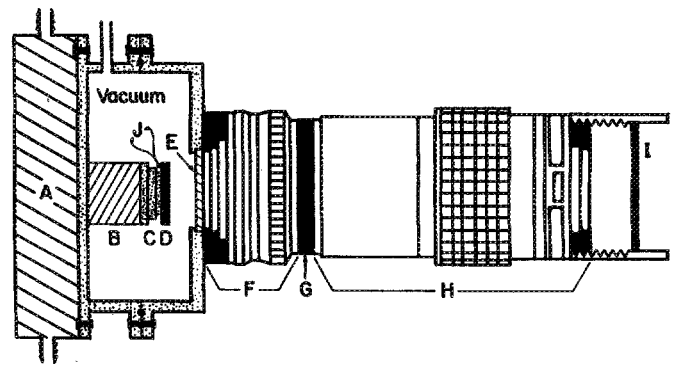

FIG. 4. Schematic view of optical coupling of CCD to phosphor screen; (A) water cooling for thermoelectric unit; (B) copper base; (C) thermoelectric cooler; (D) CCD chip; (E) quartz window; (F) 50-mm f1.2 camera lens; (G) adjustable iris; (H) 200-mm f4 camera lens; (I) phosphor screen and beryllium window; (J) thermocouple.

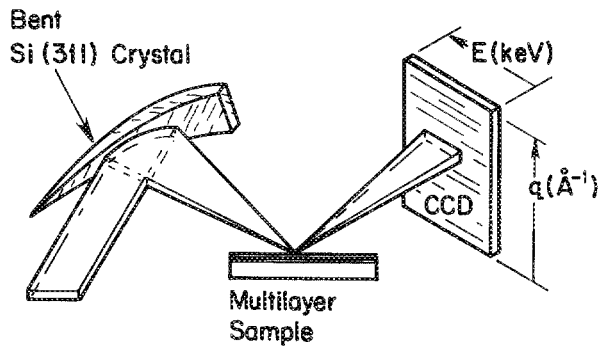

FIG. 5. X-ray optical arrangement for energy dispersive measurements.

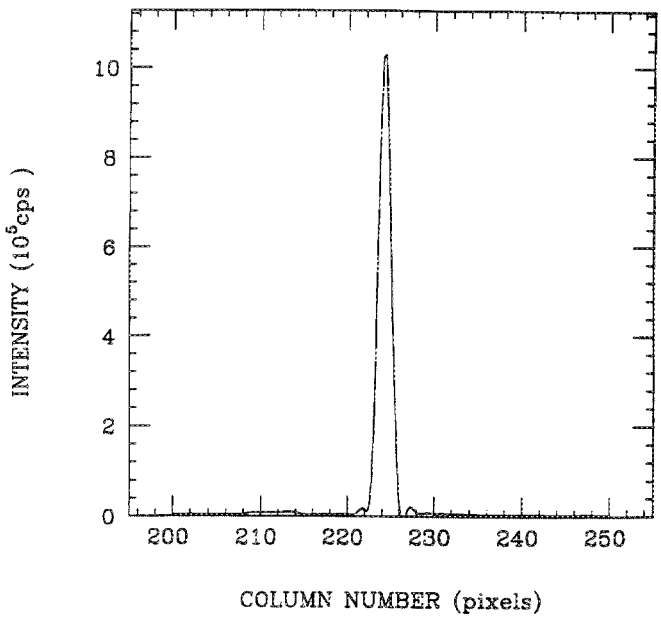

FIG. 6. CCD column readout of spatial resolution test.

crystal was adjusted to give an approximately uniform energy dispersion with a bandwidth of 400 eV.

In order to record the reflection intensity around the absorption edge, the detector was positioned so that the Pt L_{III} edge fell at about the 50th column on the CCD and then the entire 400-eV spread of energies was captured across the rows of the detector with the sample placed at the crossover point of the curved crystal. The detector was oriented to record reflectivity information in the vertical direction, thus taking advantage of the high degree of vertical collimation of the incident beam.

Most of the data were obtained with a 100 ms integration time, during which sufficiently good statistics (0.1%) could be accumulated without saturating individual pixels. The flux of the dispersed beam at the detector in this experiment was approximately 10^8 photons s^{-1} spread over an energy bandwidth of $\simeq$400 eV. Further improvement in the signal/noise can be achieved by summing over several neighboring rows with the loss of some resolution in the scattering wavevector.

V. PERFORMANCE OF THE DETECTOR: RESULTS

A variety of resolution and linearity tests were performed on the detector prior to its use in synchrotron radiation experiments. For some of these tests an LED (light emitting diode) was used as the source, triggered from the delay gate during integration mode.

Figure 6 shows a CCD image of a 150-μm wide slit illuminated by the LED with the phosphor screen removed. The observed image size of 2 pixels (45 μm) full width half maximum is consistent with the expected width of 37.5 μm, given the 4:1 reduction in image size. A similar series of tests was conducted using x rays incident on a pinhole with the phosphor screen in place, in order to check that there was no additional spreading of the image at the phosphor; no spreading of the image was observed.

In Fig. 7 we show the results of a test to determine the uniformity of the detector response over its area. With the phosphor screen removed, the detector was illuminated with white light from a translucent screen placed at the end of a 3-m tube. The inside of the tube was painted black to minimize internal reflections. The inset of Fig. 7 confirms uniform illumination to within $\pm$ 1% over a typical row slice through the pixel columns. A histogram of the number of electrons per pixel was calculated over the whole area of the chip (see Fig. 7) and, for an illumination level corresponding to $\sim$20% of saturation, the FWHM of the histogram gives a maximum pixel response variation of $\pm$ 1.5%. Note that since perfectly uniform illumination is difficult to achieve some of this variation may be due to varying light levels across the chip.

The linearity of the detector was determined by measuring the ADC output signal at different integration times ranging from 10 to 900 ms with an LED source. The plots shown in Fig. 8 indicate that the system response is linear to

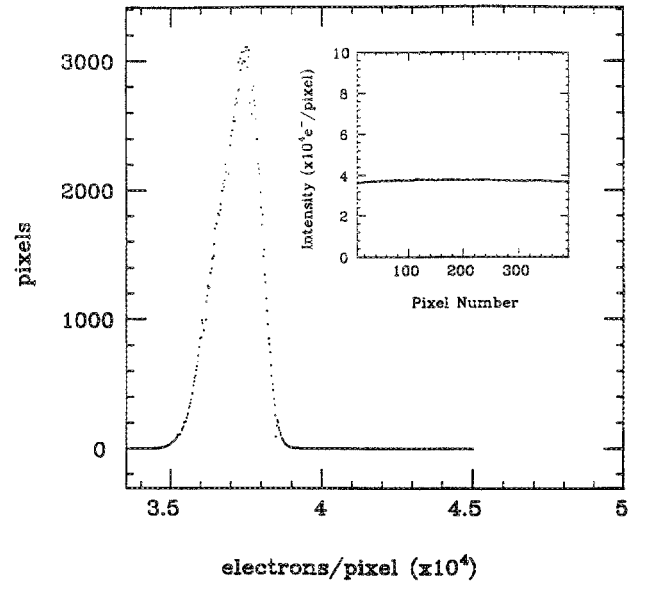

FIG. 7. Pixel response under uniform optical illumination: number of electrons per pixel histogrammed for the whole chip. Inset: pixel contents across a row slice.

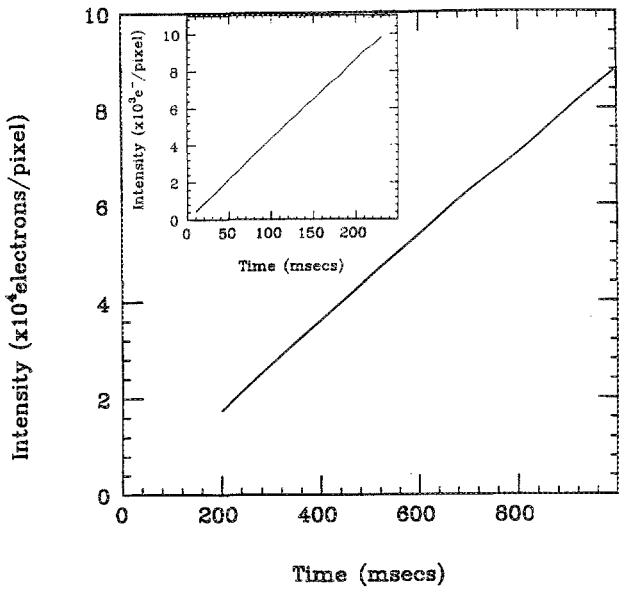

FIG. 8. Detector linearity test using optical illumination. The inset shows a blow up of the linearity at low levels of illumination (<5% of saturation).

within 0.5% over a typical operating range; the data cover the range up to 45% of saturation with the linearity at low levels of illumination (up to 5% of saturation) shown in the inset.

The next test to be carried out was the response of the CCD detector with the phosphor/lens-coupler combination in place. Two factors are important here: first, the efficiency of conversion of x-ray photons to optical photons and second, the throughput efficiency of the lens coupler. In order to measure the response of the CCD, including the optical coupling arrangement, we exposed a 7×1-mm^2 area of the phosphor with a beam of Cu$K\alpha$ (8.05 keV) x-ray photons of known flux (8×10^3 cps, as measured with a standard scintillation detector). The charge on each pixel of the CCD chip was recorded over a 10 s integration time. During this time, each pixel received on average 90 photon events. The exposed area of the phosphor screen in this test (7 mm^2) corresponds to approximately 850 pixels on the CCD, implying that $850\times90\approx7.6\times10^4$-electron-hole pairs are produced in 10 s by 8×10^4 x-ray photons. Thus, we infer a sensitivity of one electron for each x-ray photon striking the phosphor screen. The performance parameters of the detector are summarized in Table I.

TABLE I. Performance characteristics of the virtual phase CCD detector.

CCD chip	TI4849
Readout electronics	CAMAC
Frame size (pixels)	584×390
Readout noise	$20e^-$/pixel
Operating temperature	-50 °C
Quantum Efficiency ($\lambda\approx500$ nm)	0.5
Charge transfer efficiency	0.999996
Pixel well-depth	$200\,000e^-$
Linearity	<0.5%
Sensitivity (with phosphor screen and lens coupling)	$1e^-$/Xph
Spatial resolution	2 pixels
ADC resolution (12 bits)	1 in 4×10^3
Maximum dynamic range (to saturation)	10^4
Readout time	6 μs/pixel
Row parallel transfer time	50 μs
Full frame readout	1 s

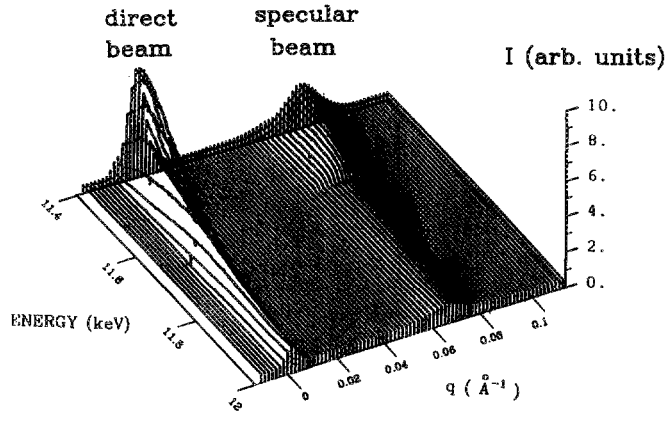

FIG. 9. CCD intensity map showing energy distribution across the Pt L_{III} absorption edge (sharp edge at ~11.6 keV on the specular beam).

Assuming a quantum efficiency of ≈0.5 for light of wavelength 500 nm, this means that each x-ray photon gives rise to two optical photons at the CCD. Of course, many more optical photons are produced by a single x-ray photon at the phosphor (~250 for this particular phosphor[16]). Losses in optical coupling, interface reflectivity, and absorption account for the difference. For some applications, such as diffuse x-ray scattering and diffraction, one would like to optimize the sensitivity of the detector. With the inefficient optical coupling mechanism employed in the current design we need ~400 x-ray photons to balance the shot noise and the electronic readout noise ($20e^-$/pixel). Deckman and

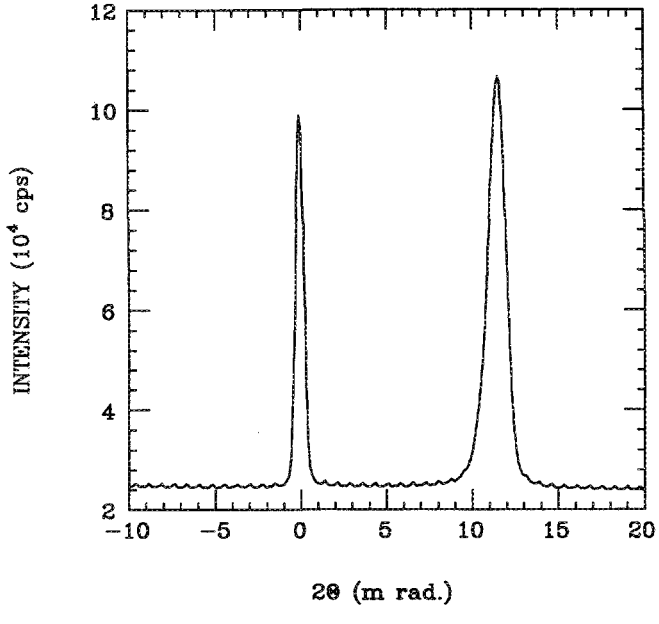

FIG. 10. Profile of specular beam ($2\theta\approx12$ mrad) from Pt-C multilayer.

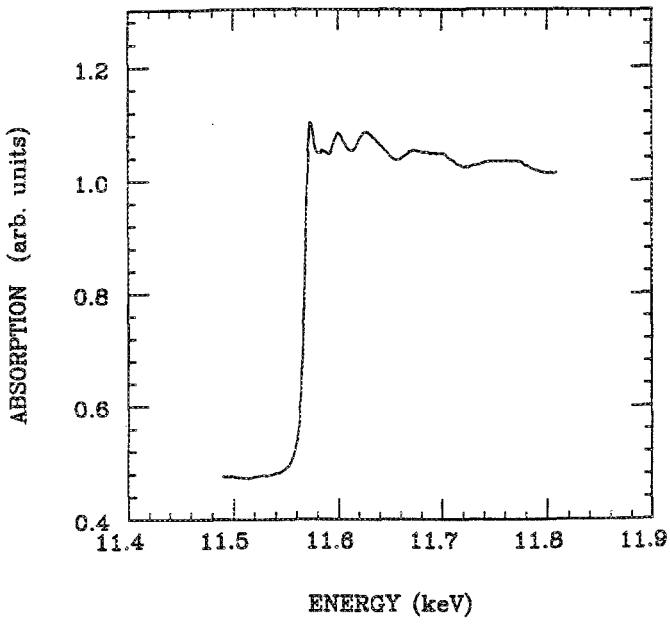

FIG. 11. Pt near-edge x-ray absorption spectrum measured using the CCD detector.

Gruner[17] have discussed the use of fiber-optic tapers as a means to reduce significantly the coupling losses. We would expect to gain an increase in sensitivity of 20–50 by replacing the lens system by a fiber-optic taper.

We should point out, however, that there are applications where a low coupling efficiency could be advantageous, for example, in the dispersive x-ray absorption measurements described in Sec. IV. In this case the detector is usually operating close to saturation. The signal-to-noise ratio then can be enhanced by reducing the shot noise produced by each x-ray photon, as would be expected as a result of low-coupling efficiency.

Finally, we describe some preliminary results which were obtained with the detector being used to record glancing-incidence reflectivity from a multilayer sample under resonant conditions, as described in Sec. IV. Figure 9 shows a two-dimensional intensity map of the CCD chip revealing the specular reflection peak together with a portion of the unscattered beam. The L_{III} absorption edge is clearly visible on the energy dispersed profile of the specular beam. The energy resolution in this data is ~ 2 eV and the wave vector resolution is 1.5×10^{-3} Å^{-1} FWHM (Fig. 10). Analysis of the Pt near-edge absorption spectrum (Fig. 11), recorded at various angles of incidence, forms the subject of a later publication.[18]

In conclusion, we have described a CCD area detector for x-ray synchrotron radiation applications. The detector is based on the "virtual phase" CCD concept which we find to be ideally suited to experiments where large dynamic range, low noise, and fast readout are required. The detector can be used either in a direct illumination mode or in conjunction with a phosphor screen and appropriate optical coupling. The optical coupling employed at present, a double lens system, is found to be inefficient for x-ray scattering experiments but can offer some advantages in single-frame recording of x-ray absorption spectra.

We have demonstrated the recording of excellent high-resolution near-edge spectroscopic and reflectivity data using energy dispersive synchrotron radiation. The detector has characteristics which are attractive for time-resolved measurements and we intend to exploit these aspects of the detector design in forthcoming experiments.

Full software control of all readout waveforms, data acquisition, and storage makes the detector easy to upgrade as new CCD chips and readout modules are introduced in this fast developing technology.

ACKNOWLEDGMENTS

It is a pleasure to thank C. Akerlof and S. Gruner for useful discussions and advice. We also thank F. Lamelas, D. Medjahed, and E. Ziegler for help in carrying out the experiments at LURE. One of us (B.R.) was supported in part by an Argonne Studentship and the research was supported by the U.S. Department of Energy, Office of Basic Energy Sciences under Contract No. W-31-109-Eng-38. RC was supported in part by NSF Low Temperature Program Grant No. DMR-8805156.

[1]See series *Handbook on Synchrotron Radiation* (North-Holland, Amsterdam, 1983 and 1987).
[2]S. M. Gruner, Science **238**, 305 (1987).
[3]See *Proceedings of the Argonne Workshop on Time-resolved Studies and Ultrafast Detectors*, Argonne, 1988. Report No. ANL/APS-TM-2.
[4]M. Wadsworth and R. D. McGrath, in *Proceedings of the 1984 International Electron Devices Meeting* (San Francisco, CA, 1984), p. 20.
[5]J. H. Kinney, Q. C. Johnson, U. Bonse, R. Nusshardt, and M. C. Nichols, SPIE Vol. **691**, 43 (1986).
[6]R. Germer, SPIE **491**, 434 (1984).
[7]W. F. Kosonocky and D. J. Sauer, in *Electronic Design* (Hayden, New York, 1975), p. 58.
[8]J. Hynecek, IEEE Trans. Electron Dev. **28**, 483 (1981).
[9]R. D. McGrath, IEEE Trans. Nucl. Sci. **NS-28**, 4028 (1981).
[10]J. R. Janesick, T. Elliott, H. M. Marsh, S. Collins, and J. K. McCarthy, Rev. Sci. Instrum. **56**, 796 (1985).
[11]Manufactured by Texas Instruments. Note that the TI4849 is no longer available and has been superseded by another virtual phase chip, TI215.
[12]C. W. Akerlof, J. W. Chapman, I. Gialas, W. A. Koska, D. F. Nitz, B. G. Rodricks, and R. S. Tschirhart, Nucl. Instrum. Methods A **260**, 80 (1987).
[13]Manufactured by 3M Industries, St. Paul, MN.
[14]Marlow Industries, Dallas, TX, Model MI3040.
[15]G. Tourillon, E. Dartyge, A. Fontaine, and A. Jucha, Phys. Rev. Lett. **57**, 603 (1986).
[16]Manufacturer's specification.
[17]H. W. Deckman and S. M. Gruner, Nucl. Instrum. Methods A **246**, 527 (1986).
[18]B. Rodricks, F. Lamelas, D. Medjahed, W. Dos Passos, R. Smither, E. Ziegler, A. Fontaine, and R. Clarke, in *Synchrotron Radiation in Materials Research*, edited by R. Clarke, J.Gland, and J. H. Weaver (North-Holland, New York, 1989).